

Adaptive Feedback Active Noise Control Headset: Implementation, Evaluation and Its Extensions

Woon S. Gan, Senior Member, IEEE, Sohini Mitra and Sen M. Kuo Senior Member, IEEE

Abstract — *In this paper, we present design and real-time implementation of a single-channel adaptive feedback active noise control (AFANC) headset for audio and communication applications. Several important design and implementation considerations, such as the ideal position of error microphone, training signal used, selection of adaptive algorithms and structures will be addressed in this paper. Real-time measurements and comparisons are also carried out with the latest commercial headset to evaluate its performance. In addition, several new extensions to the AFANC headset are described and evaluated.*

Index Terms — **Digital signal processing, active noise control headset, and real-time implementation.**

I. INTRODUCTION

As portable audio and communication devices such as MP3 players, cellular phones, PDAs, and wireless communication headsets become more widely used, designers will need to address the usage of these devices in noisy environments. Acoustic noise problems become more serious as increased numbers of industrial equipment such as engines, blowers, fans, transformers, and compressors are in use in many outdoor installations, planes, and automobiles. The traditional passive earmuffs are valued for their high attenuation over a broad frequency range; however, they are relatively large, costly, and ineffective at low frequencies. Active noise control (ANC) [1]-[3] systems cancel the unwanted noise based on the principle of superposition. Specifically, an anti-noise of equal amplitude and opposite phase is generated and combined with the primary noise, thus resulting in the cancellation of both noises. The ANC system efficiently attenuates low frequency noise, where passive methods are ineffective, bulky in size, and tend to be very expensive. ANC is developing rapidly because it permits improvement in noise reduction, which results in potential benefits in weight, volume, and cost. A better approach is to use a combination of passive and ANC technique.

Previously, analog controller using feedback configuration commonly referred to as active noise reduction [4] has been employed to cancel noise in the headsets. Since this is a non-adaptive approach, no on-line modeling of the ear-cup transfer function can be carried out in real time. Current research in ANC for communication headset focuses on using adaptive feedforward technology [2]-[3]. In practice, however, the feedforward ANC systems for headset have to handle causality

and performance deficiencies caused by non-stationary reference inputs, measurement noise, acoustic feedback [1], and higher cost of using additional reference microphones. More recently, technique has been developed to combine the analog feedback with digital feedforward [4] to achieve better noise canceling performance. However, the limited flexibility in using the analog filter can be a restriction for further improvement, such as the on-line modeling of the secondary path.

In response to the preceding problems, an adaptive feedback active noise control (AFANC) communication headset is designed. This paper is divided into three main sections. The first section gives an overview of the AFANC headset and answers some of the implementation questions. Several experiments have been conducted to model the secondary path transfer function for different error microphone positions inside the shell of the headset. In particular, we propose a broadband musical signal as the training signal for a better secondary path modeling of the headsets. The second section describes the real-time implementation of the AFANC headset using a programmable DSP processor, the evaluation of our AFANC headset with a commercial high-end active noise control headset. In the third section, an integrated approach in designing a noise reduction headset for the audio and communication applications is discussed. This integrated system not only cancels the noise for near-end listening, but also cleaned up the noise before transmitting to the far end. The performance of this integrated system is also being evaluated in term of the reduced noise level obtained.

II. ADAPTIVE FEEDBACK ACTIVE NOISE CONTROL

This section covers the structure of the AFANC, its algorithms, secondary path updates using musical signal and the ideal position of error microphone inside the headset.

A. Feedback ANC System

In an ANC application, the primary near-end noise $d(n)$ is not available during the operation of ANC because it was canceled by the secondary noise. Therefore, the basic idea of an AFANC is to estimate the primary noise, and use it as a reference signal $x(n)$ for the ANC filter, $W(z)$. Unlike an adaptive feedforward ANC system, where a separate sensor is available to pick up the reference signal, the AFANC regenerates its own reference signal. An AFANC system is required for applications include spatially incoherent noise generated from turbulence; noise generated from many

sources, and propagation paths, and induced resonance where no coherent reference signal is available.

The complete AFANC system using the filtered-x least-mean-square (FXLMS) algorithm [1] is illustrated in Fig. 1, where $\hat{S}(z)$ is required to compensate for the secondary path. The reference signal $x(n)$ is synthesized as an estimate of $d(n)$, which is expressed as

$$x(n) \equiv \hat{d}(n) = e(n) + \sum_{m=0}^{M-1} \hat{s}_m y(n-m), \quad (1)$$

where $\hat{s}_m, m = 0, 1, \dots, M-1$ are the coefficients of the M th order FIR filter $\hat{S}(z)$ used to estimate the secondary path.

The secondary signal $y(n)$ is generated as:

$$y(n) = \sum_{l=0}^{L-1} w_l(n) x(n-l), \quad (2)$$

where $w_l(n), l = 0, 1, \dots, L-1$ are the coefficients of $W(z)$ at time n , and $L-1$ is the order of the FIR filter $W(z)$. The filter's coefficients are updated by the FXLMS algorithm expressed as follows:

$$w_l(n+1) = w_l(n) + \mu x'(n-l)e(n), \quad l = 0, 1, \dots, L-1 \quad (3)$$

where μ is the step size, and

$$x'(n) \equiv \sum_{m=0}^{M-1} \hat{s}_m x(n-m) \quad (4)$$

is the filtered reference signal.

The AFANC algorithm summarized in (1) to (4) is very effective and compact since no reference sensor is required at the external of the headset. However, in some cases, large noise level difference can make the algorithm unstable. An effective solution is to employ the normalized FXLMS algorithm [1] as follows:

$$w_l(n+1) = w_l(n) + \frac{\mu}{\hat{P}_x(n) + c} x'(n-l)e(n), \quad (5)$$

for $l = 0, 1, \dots, L-1$, where the power estimate

$$\hat{P}_x(n) = (1 - \alpha) \hat{P}_x(n-1) + \alpha x^2(n) \quad (6)$$

is based on the first-order recursive filter with $\alpha \approx 0.99$, and c is a small constant to prevent using a large step size.

B. Modeling of Secondary Paths

As mentioned in the previous section, the secondary path $S(z)$ needs to be estimated and used in the updating process of the FXLMS algorithm. Estimation of $S(z)$ is usually performed off-line, followed by on-line modeling [1]. Off-line initialization is carried out initially when a training signal is injected into both the adaptive filter $\hat{S}(z)$, and the actual secondary path $S(z)$. This configuration becomes the traditional adaptive system identification. It is important to

select a training signal that is persistently excited so as to model the secondary path over the entire frequency range of interest. White noise, which has a flat spectral density for all frequencies, is commonly used as an ideal broadband training signal for system identification. In some applications, one might use bandlimited or colored noise, where the power of the signal is constant over the range of frequencies of interest, and zero elsewhere. A chirp signal can also be used for this purpose. However, for ANC headset application, where the off-line modeling signal is heard every time the AFANC headset is turned on, it is desirable to use a more soothing signal for training.

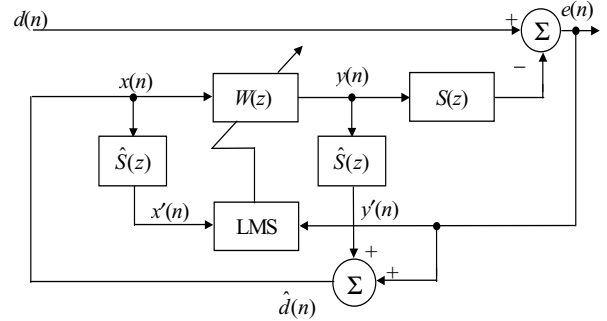


Figure 1. Block diagram of adaptive feedback ANC system

A possibility is to use music with wide bandwidth excitation to model the secondary path over a period of time. Since the standard sampling frequency for communication applications is 8 kHz, any ideal training signal specific to such applications should have a flat spectrum in the 0 to 4 kHz frequency range. Thus, the first step is to search for a musical piece with rich frequency content in the 0 to 4 kHz frequency range. However, the challenge is to find a musical piece that has constant signal envelope over the period of training. We found that an opera piece from "O Fortuna from Carmina Burana," [5] consists of a number of consecutive frames that are rich in frequency content as shown in Fig. 2. A power spectrum analysis on these cumulative frames showed it to be almost flat in the frequency range from 0-1700 Hz. After this range, the spectrum slowly sloped down up to 4 kHz. Thus, it was decided that equalization be applied to the upper frequency (using highpass filter with cutoff frequency at 1.7 kHz, followed by 10 dB of amplification) of this musical piece to give a flat frequency response for the 0-4 kHz frequency range.

In order to test the effectiveness of the equalized music signal as a training signal, white noise was replaced by the equalized music piece in the off-line secondary-path modeling algorithm. Figure 3 shows the estimated filter coefficients of the secondary-path filter, $S(z)$, obtained using musical signal and white noise for off-line modeling. The system modeling capability of the chosen musical signal is as good as the white noise.

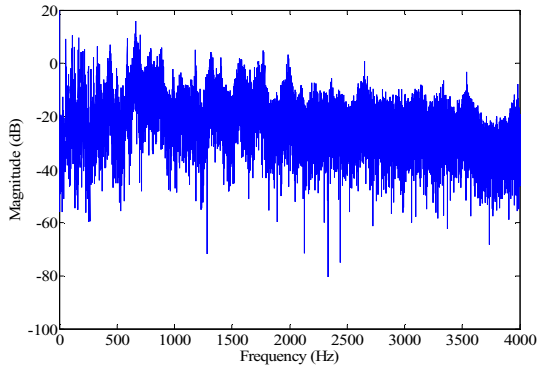


Figure 2. Power spectrum of the music piece from “O Fortuna from Carmina Burana.”

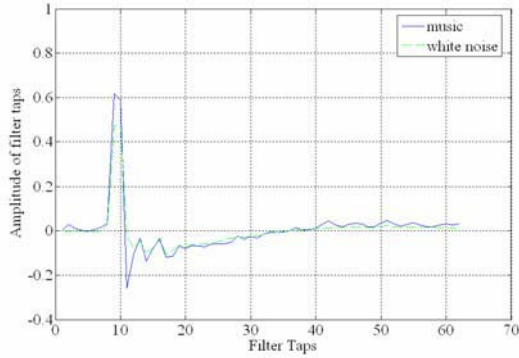


Figure 3. Estimated secondary-path filter coefficients for $\hat{S}(z)$ using music signal and white noise for off-line modeling.

After the off-line modeling, the AFANC system can be operated without the need to continuously update the $\hat{S}(z)$. However, on-line modeling of $S(z)$ can still be performed to keep track on the changes of $S(z)$ due to slight movement of the headset. In Section 4, we will describe how on-line modeling can be carried out using speech signal.

C. Ideal Position of the Error Microphone

The position of the error microphone used in the AFANC headset can have a great impact on the secondary path modeling. This is due to the fact that sound generated by the secondary emitter (speaker) in the headset directly hits the ear's pinna, which is the external portion of the ear. The sound from the emitter undergoes changes in its spectral content, due to the filtering effects of sound hitting the pinna.

Therefore, the primary objective behind this study is to find an optimum error microphone location inside the ear-cup for the ANC application. In this section, we will carry out a series of measurements to identify secondary path transfer functions at different positions. A control systems analyzer was used to generate the random noise for estimating the poles and zeros of the secondary path transfer function from the headphone emitter (loudspeaker) to the error microphone. The headphone

system used is a circumaural headsets which was mounted on a KEMAR (Knowles Electronics Mannequin for Acoustics Research) mannequin. A stereo amplifier was used to amplify the source signal being fed from the control system analyzer to the headphone loudspeaker. The error signal was picked up by an omnidirectional Realistic electret tie pin microphone embedded inside the ear-pads of the headphone. The microphone signal was pre-amplified by a dual microphone preamplifier before it reached the control system analyzer input. The sampling frequency chosen was 8 kHz, the frequency range of interest being between 0 to 3 kHz.

The pinna-related measurement is taken at eight different error microphone locations [5] on the median plane around the ear-pad of the headphone mounted on the KEMAR as shown in Fig.4. In particular, we noted that the worst transfer function occurs at position #2, with many peaks and nulls. The best transfer function with the fewest peaks and nulls occurs at position #8. The problem with transfer function with many peaks and nulls are its difficulty in adapting to such a system during offline modeling. Their frequency responses at position #2 and #8 are plotted in Fig. 5.

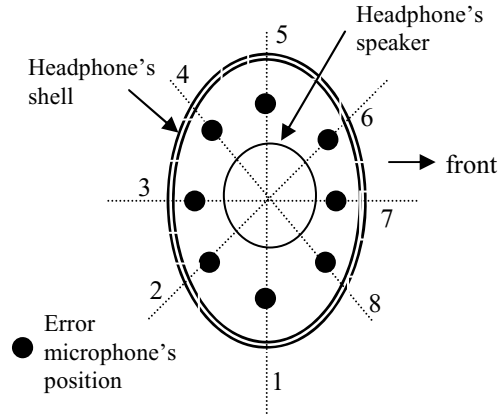


Figure 4. Eight different microphone locations on the right ear-pad.

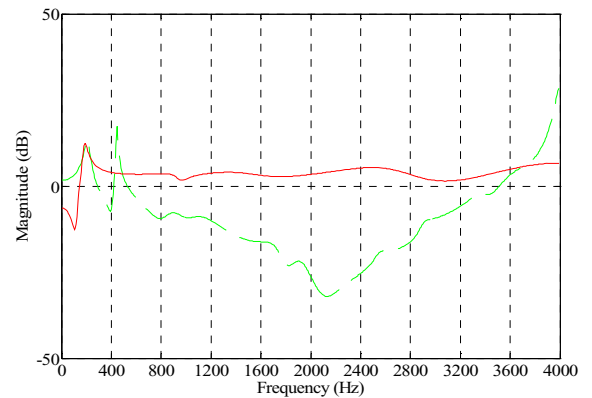


Figure 5. Frequency responses of $S(z)$ at microphone locations #8 (solid line) and #2 (dotted line).

In addition, we also measured the frequency response of $S(z)$ using the microphone located at the right ear cavity of the KEMAR. This measurement produces a very flat frequency response, which is ideal for the development of the AFANC headset. However, it is not practical and uncomfortable to insert an error microphone inside the ear canal of the listener. Coincidentally, the measurement results [5] also shown that microphone placed at the frontal positions (#6, #7, #8) produces the flattest response among the 8 positions. Since the position #8 is very near the external auditory meatus, the microphone could fit in more easily inside the hollow in that location unlike the position #6 where cartilaginous framework could pose a problem. Moreover, an added advantage is that at this location (#8), the microphone is at one of the nearest possible positions to the ear canal. Therefore, the ideal position at found at position #8, which has the flattest frequency response and at position closed to the ear canal among the 8 positions.

III. REAL-TIME IMPLEMENTATION AND EVALUATION OF PERFORMANCE

A. Real-Time Implementation

In the real-time implementation of the AFANC headset, the error signal $e(n)$ was picked up by an omni-directional electret microphone embedded inside the ear-pads of the headphone system. The headphone was mounted on a KEMAR mannequin. The error signal was pre-amplified by a dual preamplifier and sent to the DSP system. The anti-noise $y(n)$ generated by the DSP was amplified by a stereo amplifier, before it was sent to the secondary loudspeaker mounted on the headphone system. The engine noise was played from a Sony digital audio tape (DAT) deck, pre-amplified by an amplifier and played from a speaker, which faced the KEMAR, 27 cm in front and 24 cm below as shown in Fig. 6.



Figure 6. Primary loudspeaker positioned in front of KEMAR

The DSP algorithms were implemented on a programmable floating-point digital signal processor. This processor can handle 32-/40-bit floating-point operations. A daughter module was used as a peripheral device for interfacing the DSP processor with real-world analog signals. The sampling frequency for the 16-bit A/D converters was software programmed to 8 kHz and the cut off frequency of the analog anti-aliasing lowpass filter on the daughter module is 3.2 kHz. The AFANC algorithm was coded in assembly language and debugged using the debugger.

With the error microphone placed at the optimum microphone location, discussed previously in Section II-C, noise cancellation tests were conducted for different primary noises [5]. The length of the filter L for off-line modeling of the secondary path was fixed at 65, the step size parameter is set at 0.05; the length of the adaptive filter $W(z)$ used for the on-line cancellation was set at 110. The measurements are carried out over a period of 4 seconds (or 32,000 iterations at sampling frequency of 8 kHz).

B. Performance Evaluation

In this section, we investigate the performance of the AFANC using white training noise and equalized musical signal for off-line secondary-path modeling. Two engine noises recorded at 2,200 rpm and 3,700 rpm are used as the primary noise to test the performance of the AFANC. At 2,200 rpm, there are four dominant narrowband noise components at harmonics 76 Hz, 116 Hz, 156 Hz and 196 Hz; whereas at 3,700 rpm, narrowband components are at 61 Hz, 122 Hz and 183 Hz. The noise reduction capability of the AFANC (using white noise as training signal) is measured and plotted in Fig. 7 for engine noise recorded at 2,200 rpm. The average noise reduction over the four noise harmonics is around 15.424 dB. In the case of 3,700 rpm, the average noise reduction over the three harmonics is around 23.27 dB.

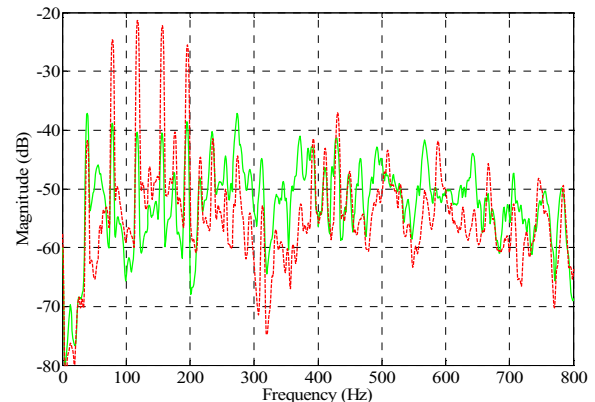


Figure 7. Power spectrum for engine noise (dotted line) and residual error (solid line) at 2,200rpm

Instead of using white noise as the training signal, we next examine the noise reduction performance using the equalized musical source in Section II-B. The average noise reduction for the noise harmonics in 2,200 rpm and 3,700 rpm are

around 10 dB and 15.2 dB, respectively. Therefore, a slight drop of 5-7 dB is observed using the equalized musical training signal over the white noise training signal.

In the final performance evaluation, we compare the AFANC headset against a high-end commercially available noise canceling headset. For consistent comparison, the noise cancellation performances for both headsets were monitored by the KEMAR microphone embedded in the KEMAR's ear. The net noise attenuation of the proposed AFANC and the commercial available noise headset are shown in the bar diagrams of Fig. 8 for 2,200 rpm and 3,700 rpm. It is shown that the proposed AFANC headset has very good low-frequency cancellation capability compared to the commercial available headset. In addition, we also measured the passive noise cancellation (by turning off the active noise cancellation feature) performance of both headsets and found that both headsets give a comparable and good level of high frequency (above 2 kHz) attenuation.

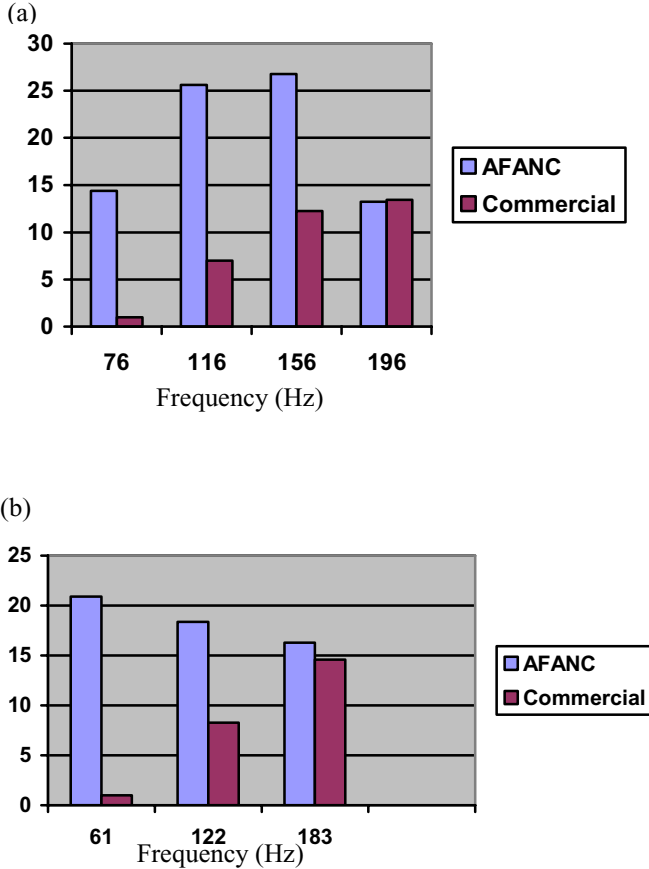


Figure 8. Net noise cancellation comparison for the proposed AFANC and a commercial noise canceling headset for engine noise at (a) 2,200 rpm and (b) 3,700 rpm

IV. EXTENSION OF AFANC

A. Integrated Feedback Active Noise Control

We can further integrate the above AFANC with the receiving audio input to form an integrated adaptive feedback active noise control (IAFANC) system [5]. In IAFANC, the residual noise picked up by the error microphone is used to synthesize the primary noise $x(n)$ for updating the adaptive filter coefficients using the FXLMS algorithm. Since the IAFANC is integrated with the existing audio playback systems (such as walkman or MP3 players) or communication headset, the microphone placed inside the ear cup picks up both the residual noise and the desired audio signal. However, the audio components will also become the interference to the IAFANC algorithm and a method is devised to neatly combine the audio and the ANC system.

In this section, we introduce the detailed integration of AFANC [6] with the audio system as shown in Fig. 9. The error sensor output signal, $e(n)$, contains the residual noise plus the desired audio signal. The audio interference cancellation filter, $\hat{S}(z)$, uses the audio signal, $a(n)$, as the reference signal to estimate and then remove the audio components in $e(n)$. The difference error signal, $e'(n)$, consists only of the residual noise, is used to update the adaptive noise control filter, $W(z)$. Note that the updating of $\hat{S}(z)$ using the LMS algorithm can be conducted off-line using a wideband musical signal as explained in Section II-B and followed by using the audio signal as the reference input to adjust the weights on-line. However, the step size used in on-line modeling must be kept small so as to adapt effectively to the small changes of $S(z)$.

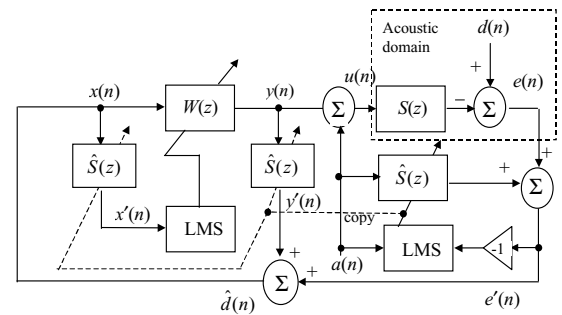


Figure 9. An integrated audio and ANC system

Assuming that the audio signal $a(n)$ is of persistent excitation and uncorrelated with the primary noise $d(n)$, the secondary path $S(z)$ can be modeled on-line by the audio interference cancellation filter $\hat{S}(z)$. After $\hat{S}(z)$ has converged, we obtained the difference error and the error respectively as

$$E'(z) = E(z) + \hat{S}(z)A(z), \quad (7)$$

$$E(z) = D(z) - U(z)S(z). \quad (8)$$

Substituting (8) into (7), we obtain

$$E'(z) = D(z) - U(z)S(z) + \hat{S}(z)A(z). \quad (9)$$

Since $U(z) = A(z) + Y(z)$, therefore (9) becomes

$$E'(z) = D(z) - A(z)S(z) - Y(z)S(z) + \hat{S}(z)A(z). \quad (10)$$

The optimal solution for the audio interference cancellation filter is $\hat{S}(z) = S(z)$, therefore, (10) becomes

$$E'(z) = D(z) - Y(z)S(z). \quad (11)$$

Equation (11) shows that the $E'(z)$ is reduced to the residual error of ANC system, where the primary noise $D(z)$ is cancelled by the anti-noise $Y(z)S(z)$. Note that

$$X(z) = E'(z) + Y(z)\hat{S}(z). \quad (12)$$

Comparing (11) and (12), resulted in $D(z) = X(z)$ if $\hat{S}(z) = S(z)$. That is, we obtain an accurate reference signal for the noise control filter $W(z)$.

B. IAFANC with Adaptive Noise Cancellation

In speech communication, there is also a need to remove the near-end noise before sending it to the far-end. As shown in Fig. 10, a simple adaptive noise canceling filter $H(z)$ with the LMS algorithm can be used to remove the near-end noise. The microphone used to pick up the desired near-end signal also sensed the undesired near-end noise. $P(z)$ is the primary path from the noise source to the microphones. However, a correlated noise input must be used to train the noise canceling filter $H(z)$ using the LMS algorithm. The adaptive LMS algorithm is given as:

$$h_l(n+1) = h_l(n) + \mu y(n-l)e(n), \quad l = 0, 1, \dots, L-1 \quad (13)$$

where $y(n)$ is correlated with the reference near-end noise.

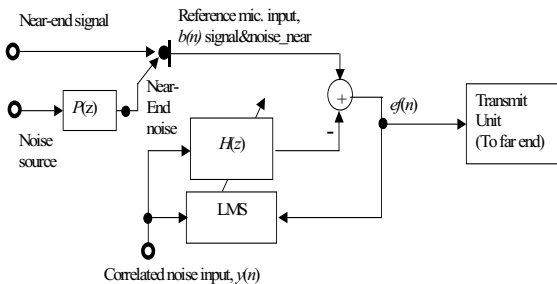


Figure 10. Adaptive noise cancellation filter for far-end transmission

This section describes the integration of the feedback ANC filter $W(z)$, the secondary path modeling filter $\hat{S}(z)$, and the adaptive noise canceling filter $H(z)$. Altogether, three microphones are used in this integrated ANC-communication headset. One microphone is placed close to the emitter inside each ear-cup as shown in Section II-C. These microphones are

assigned as the error microphones to pick up the noise entering the ear-cup. A communication microphone, which is located external of the ear-cup, is used to pick up the near-end speech, but corrupted by the near-end noise.

In the proposed integrated ANC-communication system [7], the residual noise picked up by the error microphone is used to synthesize the primary noise $x(n)$ for updating the adaptive filter coefficients using the FXLMS algorithm. The far-end speech component will also become the interference to this integrated system, and a method is developed to combine the communication and the ANC systems.

The detailed integration of adaptive feedback ANC with communication system is shown in Fig. 11. The error sensor output signal $e(n)$ contains both the residual noise and the desired speech signal. The speech interference cancellation filter $\hat{S}(z)$ uses the far-end speech signal $a(n)$ as the reference signal to estimate and then remove the speech components in $e(n)$. The difference error signal, $e'(n)$, consists of the residual noise only, is used to update the adaptive noise control filter $W(z)$. Note that the update of $\hat{S}(z)$ using the LMS algorithm is located at the output of the feedback ANC, and can be used for both off-line and on-line modeling as explained in the previous section.

It has been shown analytically in the previous section that the regenerated reference signal $x(n)$ derived from the adaptive filter $W(z)$ and the error signal, is a close estimate of the primary noise $d(n)$. That is, we are able to obtain an accurate reference signal for the noise control filter $W(z)$. The noise cancellation filter $H(z)$ can be neatly integrated into the system by channeling the anti-noise signal $y(n)$ into its input. The signal $y(n)$ is highly correlated to the near-end noise $d(n)$, and therefore it is a good candidate for the input of $H(z)$. This filter provides good cancellation of the near-end noise to produce a cleaner near-end speech for transmission. Furthermore, no additional microphone is required to pick up the reference noise, thus solving the crosstalk interference between microphones.

We can summarize several advantages of the integrated ANC-communication system as follows: (1) good estimation of the true residual noise $e'(n)$ without interfering with the speech signal $a(n)$; (2) large step size can be used in adapting the cancellation filter $W(z)$ since the difference error signal $e'(n)$ used by the FXLMS algorithm is not corrupted by the high volume speech signal; (3) the adaptive feedback ANC technique provides a more accurate noise cancellation since the microphone is placed inside the ear-cup of the headset; (4) the system uses single microphone per ear cup, thus produces a compact, lower power consumption, and a cheaper solution; (5) the audio signal can be neatly used to drive both on-line and off-line modeling of the secondary path transfer function; and (6) the use of adaptive noise cancellation filter enhances the near-end speech before sending to the far-end. The next section will examine some of the performance results obtained using this integrated system.

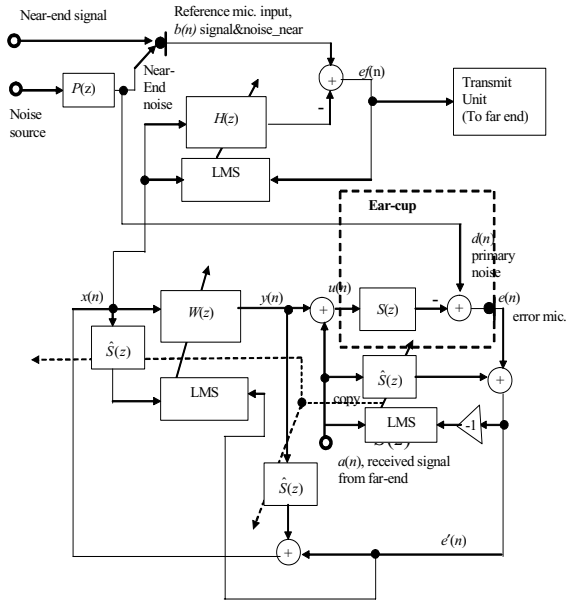


Figure 11. An integrated communication and ANC system.

C. Performance of IAFANC with Adaptive Noise Cancellation

Computer simulation was conducted to examine the combined performance of the integrated ANC-communication headset. The impulse response of the headset was measured using a dummy head, and recorded speech and noise signals were used in these computer simulations.

Experiment was carried out in order to evaluate the capabilities of the integrated system. An engine noise with prominent harmonics at 61 Hz, 122 Hz and 183 Hz was used as the noise source. The adaptive filters $W(z)$, $H(z)$, and $\hat{S}(z)$ used in this simulation are 128-tap, 64-tap, and 80-tap FIR filters, respectively. Step sizes of 0.01, and 0.05 were used to adapt $W(z)$ and $H(z)$ respectively. Off-line modeling of $S(z)$ was first performed to obtain the secondary path estimation $\hat{S}(z)$ by using a wide spectrum musical signal with a step size of 0.01, and followed by on-line modeling using the speech signal with a small step size of 0.0005.

Figure 12 shows the case when the speech signal was corrupted by the engine noise. Note that the engine noise was recorded from the welding power generator running at 3,700 rpm. The narrowband harmonics (61 Hz, 122 Hz, and 183 Hz) were canceled by more than 30 dB. Figure 13 shows the original signal corrupted by engine noise, and the enhanced near-end signal after passing through the adaptive filter. The near-end speech signal was enhanced by more than 25 dB.

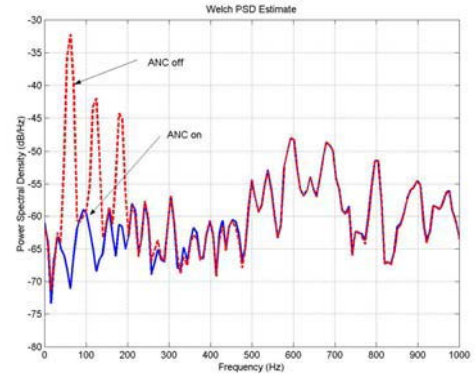


Figure 12. Noise spectral for the error signals without (dotted line) and with (solid line) using ANC filter under an engine disturbance.

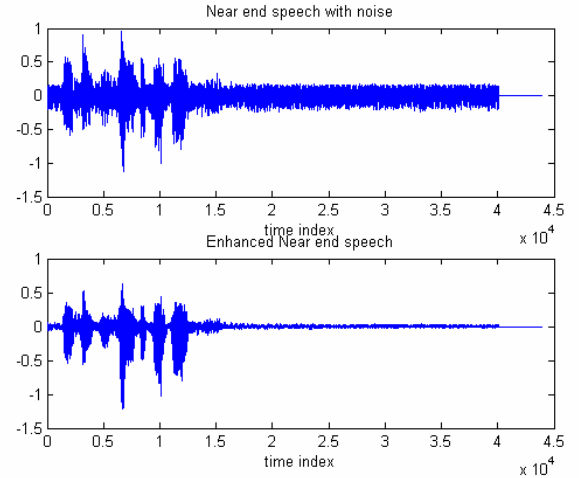


Figure 13. The top and bottom plots show the original signal corrupted by engine noise and enhanced near-end speech respectively

V. CONCLUSIONS

In this paper, we presented several topics on the AFANC system. These topics include the structure of the AFANC, its adaptive algorithm, using musical signal to model the secondary path, finding the ideal position of the error microphone, its real-time implementation, its performance evaluation with a commercial active noise control headset, and its extension for a clearer speech communication.

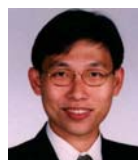
Several important findings have been obtained which includes: (a) optimum position of the error microphone for AFANC headset, (b) ability to use a wide spectrum musical signal for off-line modeling of the secondary path, (c) integration of AFANC into existing audio and communication system, (d) good performance of the AFANC headset and its performance has also been evaluate against existing commercial noise canceling headset.

Overall, the strength of the AFANC headsets is its good noise estimation using a single microphone inside each ear-cup of the headset. Its also has a nice structure to integrate neatly to existing speech-communication devices, like cell phones.

References

- [1] Sen M. Kuo and Dennis R. Morgan, *Active noise control systems: Algorithms and DSP implementations*, John Wiley & Sons, Inc., New York, 1996.
- [2] C. H. Hansen and S. D. Snyder, *Active control of noise and vibration*, E&FN Spon, London, 1997.
- [3] B. Widrow and E. Walach, *Adaptive inverse control*, Prentice Hall, Upper Saddle River, NJ, 1996.
- [4] B. Rafaely, Active noise reducing headset, OSEE Online Symposium, 2001, pp 1-8.
- [5] Sohini Mitra, *Adaptive Feedback Active Noise Control Headset*, MS Thesis, Northern Illinois University, DeKalb, IL, 2004.
- [6] W. S. Gan and Sen M. Kuo, "An integrated audio active noise control headset", *IEEE Transaction on Consumer Electronics*, Vol. 48, No. 2, May 2002, pp 242-247.
- [7] W. S. Gan and Sen M. Kuo, "Integrated Active Noise Control Communication Headset", In Proc. of *International Symposium on Circuits and Systems*, May 25 - 28, 2003, pp. IV353-356.

BIOGRAPHY



Woon-Seng Gan (M '93, SM '00) received his B.Eng (1st Class Hons) and PhD degrees, both in Electrical and Electronic Engineering from the University of Strathclyde, UK in 1989 and 1993 respectively. He joined the School of Electrical and Electronic Engineering, Nanyang Technological University, Singapore as a Lecturer in 1993. Currently, he is an Associate Professor. His research interests include adaptive signal processing, psycho-acoustic signal processing and real-time DSP implementation. He has recently co-authored a book on "Digital Signal Processors: Architectures, Implementations, and Applications", (Prentice Hall, 2005).

Sohini Mitra received her MSEE degree from Northern Illinois University in 2004. She is currently with Motorola Inc. IL.



Sen M. Kuo (M '85, SM '04) received the B.S. degree from National Taiwan Normal University, Taipei, Taiwan, in 1976 and the M.S. and Ph.D. degrees from the University of New Mexico in 1983 and 1985, respectively. In 1993, he was with Texas Instruments, Houston, TX. He is currently a Professor and Chair at the Department of Electrical Engineering, Northern Illinois University, DeKalb, IL. He is the author of *Active Noise Control Systems: Algorithms and DSP Implementations* (New York: Wiley, 1996), *Real-Time Digital Signal Processing* (Wiley, 2002), *Digital Signal Processors: Architectures, Implementations, and Applications* (Prentice Hall, 2005), and of numerous technical papers. He has been awarded seven US patents. His research focuses on active noise and vibration control, adaptive echo and noise cancellation, digital audio applications, and digital communications.